Factor Graph Based Simultaneous Localization and Mapping Using Multipath Channel Information

Erik Leitinger[†*], Florian Meyer[‡], Fredrik Tufvesson[†], and Klaus Witrisal[*]

[*]Graz University of Technology, Graz, Austria ({erik.leitinger,witrisal}@tugraz.at)
[†]Lund University, Lund, Sweden (fredrik.tufvesson@eit.lth.se)
[‡]Massachusetts Institute of Technology, Cambridge, MA, USA (fmeyer@mit.edu)

***Abstract*—Radio-based localization has the potential to provide centimeter-level position information. In this paper we apply joint probabilistic data association to multipath-assisted simultaneous localization and mapping (SLAM) for this purpose. In multipath-assisted localization, position-related information in multipath components (MPCs) is exploited to increase the accuracy and robustness of indoor tracking. Based on a recently introduced loopy belief propagation multipath-assisted localization scheme that performs probabilistic data association jointly with agent state estimation, we build a method for SLAM without using a-priori known environment maps. The proposed method is highly accurate and robust in localizing a mobile agent while building up an environment feature map. It scales well in all relevant systems parameters and has a very low computational complexity.**

I. Introduction

The purpose of simultaneous localization and mapping (SLAM) [1] is to estimate an agent's pose (including its position) and the surrounding environment using uncertain data. SLAM algorithms have to process two types of uncertainties: (i) unknown associations between measurements and their respective origins and (ii) (possibly a-priori unknown) sensor uncertainties for weighting the measurements accordingly.

Feature-based SLAM is a variant of SLAM where landmarks in a map are estimated and used instead of the map itself. In general, there are two major classes of feature-based SLAM approaches, (a) vector-based feature mapping [1] and (b) set-based feature mapping [2], [3]. Vector-based approaches apply data association (DA) and subsequent Bayesian filtering meaning that the uncertainties in (i) and (ii) are somehow separated from each another. Set-based approaches comprise both types of uncertainties in (i) and (ii) in a Bayesian approach using finite set statistics (FISST) and random finite sets (RFS) [4]. A new class of FISST-based filters that are applied on multitarget tracking, but also have high potential for SLAM, include [5]–[7]. In particular, an application of the labeled multi Bernoulli filter [6] to SLAM has been introduced in [8].

Multipath-assisted indoor navigation and tracking (MINT) exploits position-related information in multipath components (MPCs) of the radio channel that can be associated with the local geometry [9], [10]. It thus turns multipath propagation from an impairment into an advantage. Using ultra-wideband (UWB) transmit signals, specular MPCs are estimated from the received signals and used for positioning and tracking. This is accomplished by associating the estimated MPC delays with delays modeled by to the geometric distance between the mobile agent and a physical anchor or a corresponding virtual source referred to as *virtual anchor* (VA). Thus, each MPC corresponds to a physical anchor or to a VA. The VA positions are mirror images of the positions of the physical anchors as illustrated in Fig. 1; they can be obtained by using a-priori knowledge of the floor plan or a simultaneous-localization-and-mapping approach [11]–[13]. A critical step of MINT is the DA between the estimated delays of MPCs and the anchors (both physical anchors and VAs) [10]. To overcome robustness issues in situations where the MPC-feature associations are ambiguous, i.e. when path-overlap of MPCs occurs, we have introduced a joint probabilistic data association (JPDA) method [14] in [15] using belief propagation (BP) [16], [17].

In this paper, we propose an algorithm for feature-based SLAM with ordered vectors based on the multitarget-multisensor methods presented in [17], [19], [20], which

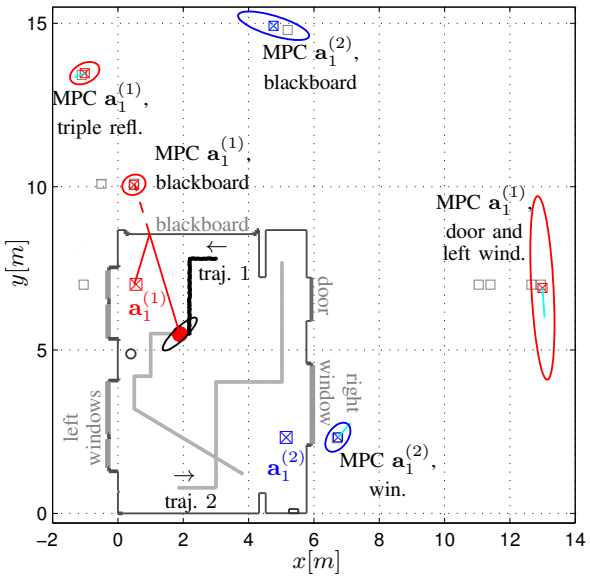

Fig. 1. Illustration of the environment map [18] obtained by the multipath-assisted SLAM algorithm. Two physical anchors at $\mathbf{a}_1^{(1)}$ and $\mathbf{a}_1^{(2)}$ represent the infrastructure. The gray dotted-lines represent the measured trajectories (traj. 1 and 2) along which the mobile agent is moving. Gray squares indicate geometrically expected VAs, blue and red plus markers with uncertainty ellipses (40-fold) represent discovered VAs. An agent tracking result is shown in black with a corresponding error ellipse (100-fold).

This work was supported by a grant from the Swedish foundation for strategic research (SSF) and by the Austrian Science Fund (FWF) under grant J3886-N31.

apply BP-based JPDA on multitarget-multisensor setups. The new algorithm extends the method in [15] to SLAM using multipath channel information [11], [13]. This method jointly applies data association and infers the states of the agents as well as the map features. Therefore, uncertainties of types (i) and (ii) are considered. Further, as presented in [17], the proposed method adapts the probabilities of detection to tracked map-features and accordingly chooses the measurement variances for updating the map-feature state with new incoming measurements. The key contributions of this paper are:

- A BP-based JPDA method, applied to feature-based SLAM using multipath channel information.
- An extension of the adaptive detection probability method [17] to also adapt the measurement standard deviations.
- An analysis of the presented method using real UWB data measured in an indoor environment.

The paper is organized as follows: Section II discusses the basic signal model and MPC parameter estimation. Section III introduces the system model and provides a statistical formulation of the SLAM problem. In Section IV, the proposed BP algorithm and the factor graph are described. Sections V and VI wrap up the paper with experimental results, conclusions, and a future perspective.

II. Measurement Model

A. Signal Model

Our signal model is the following. During time step n, a baseband radio signal $s(t)$ is transmitted from the j-th physical anchor located at position $\mathbf{a}_1^{(j)} \in \mathbb{R}^2$, $j \in \{1,\dots,J\} = \mathcal{J}$, to a mobile agent at position $\mathbf{p}_n \in \mathbb{R}^2$. The corresponding received signal is given as [9]

$$r_n^{(j)}(t) = \sum_{k=1}^{K_n^{(j)}} \alpha_{k,n}^{(j)} s\big(t-\tau_{k,n}^{(j)}\big) + s(t) * \nu_n^{(j)}(t) + w(t). \quad (1)$$

Here, the first term describes the contributions from $K_n^{(j)}$ specular MPCs with complex amplitudes $\alpha_{k,n}^{(j)}$ and delays $\tau_{k,n}^{(j)}$, where $k \in \big\{1,\dots,K_n^{(j)}\big\} = \mathcal{K}_n^{(j)}$. The delays $\tau_{k,n}^{(j)}$ correspond to the distances between the agent and the j-th physical anchor (for $k=1$) or the VAs of the j-th physical anchor (for $k \in \big\{2,\dots,K_n^{(j)}\big\}$). Thus, $\tau_{k,n}^{(j)} = \big\|\mathbf{p}_n - \mathbf{a}_k^{(j)}\big\|/c$, where $\mathbf{a}_k^{(j)} \in \mathbb{R}^2$ is the position of the respective (physical or virtual) anchor[1] and c is the speed of light. The energy of the transmitted signal $s(t)$ is assumed to be normalized to one. The second term in (1) denotes the convolution of $s(t)$ with the diffuse multipath (DM) $\nu_n^{(j)}(t)$, which is modeled as a non-stationary zero-mean Gaussian random process. Considering uncorrelated scattering along the delay axis τ, the auto-correlation function of $\nu_n^{(j)}(t)$ is given by $\mathbb{E}_\nu\big\{\nu_n^{(j)}(\tau)\nu_n^{(j)*}(u)\big\} = S_{\nu,n}^{(j)}(\tau)\delta(\tau-u)$, where $S_{\nu,n}^{(j)}(\tau)$ represents the power delay profile of DM. The DM process $\nu_n^{(j)}(t)$ is assumed to be quasi-stationary in the spatial domain, which means that $S_{\nu,n}^{(j)}(\tau)$ does not change in the vicinity of $\mathbf{p}_n$ [21]. Note that the DM component interferes with the useful position-related information. The last term in (1), $w(t)$, is additive white Gaussian noise with double-sided power spectral density $N_0/2$.

[1]From now on physical anchors and VAs are referred to as map features, if not stated otherwise.

B. MPC Parameter Estimation

The delays of the MPCs at agent position $\mathbf{p}_n$ are estimated recursively by a least-squares approximation of the received signal [22]. The algorithm estimates up to a predefined maximum number M of MPCs yielding estimated delays $\hat{\tau}_{m,n}^{(j)}$ and according complex amplitudes $\hat{\alpha}_{m,n}^{(j)}$, with $m \in \{1,\dots,M_n^{(j)}\} = \mathcal{M}_n^{(j)}$. The estimated delays are scaled by the speed of light c and used as noisy distance measurements $z_{m,n}^{(j)} = c\hat{\tau}_{m,n}^{(j)}$ in the proposed multipath-assisted SLAM algorithm. Furthermore, in a real-world MINT system, the amplitude estimates $\hat{\alpha}_{m,n}^{(j)}$ (after being associated with the k-th anchor) are fed into a higher-level, non-Bayesian algorithm that determines the signal-to-interference-plus-noise power ratio (SINR) between the useful specular MPC and the DM plus noise. This SINR is related to the range standard deviation $\sigma_{m,n}^{(j)}$ (see [10], [22] for details). Note that an extension to additional parameters besides the delay (and the corresponding amplitude), as for example the angle-of-arrival and angle-of-departure of the MPCs, is straightforward.

III. System Model and Statistical Formulation

The used formulation follows closely [15], [17], [19], [20], where the work in [15] presents a JPDA-MINT algorithm with the a-priori assumption of perfect map knowledge. This assumption is relaxed in the following problem formulation.

A. Agent, Feature, Measurement, and Association Vectors

The state of the mobile agent at time n is described by $\mathbf{x}_n = [\mathbf{p}_n^{\mathrm{T}}, \mathbf{v}_n^{\mathrm{T}}]^{\mathrm{T}}$, where $\mathbf{v}_n$ is the velocity. The state evolves over time n according to a prescribed state transition probability density function (pdf) $f(\mathbf{x}_n|\mathbf{x}_{n-1})$. There are $K_n^{(j)}$ features and the existence of the (j,k)-th feature is indicated by $r_{k,n}^{(j)} \in \{0,1\}$, where $r_{k,n}^{(j)} = 1$ means that it exists at time n. The state of the (j,k)-th feature is described by its position $\mathbf{a}_{k,n}^{(j)}$. The augmented feature state is defined as $\mathbf{y}_{k,n}^{(j)} = [\mathbf{a}_{k,n}^{(j)\mathrm{T}}, r_{k,n}^{(j)}]^{\mathrm{T}}$ [19]. We also define the stacked vectors $\mathbf{y}_n^{(j)} = [\mathbf{y}_{1,n}^{(j)\mathrm{T}}, \dots, \mathbf{y}_{K_n^{(j)},n}^{(j)\mathrm{T}}]^{\mathrm{T}}$, $\mathbf{y}_n = [\mathbf{y}_n^{(1)\mathrm{T}}, \dots, \mathbf{y}_n^{(J)\mathrm{T}}]^{\mathrm{T}}$, $\mathbf{r}_n^{(j)} = [r_{1,n}^{(j)}, \dots r_{k,n}^{(j)}]^{\mathrm{T}}$ and $\mathbf{r}_n = [\mathbf{r}_n^{(1)}, \dots \mathbf{r}_n^{(J)}]^{\mathrm{T}}$.

The MPC distances described in Section II-B are subject to a data association uncertainty, i.e., it is not known how the mobile agent's measurements $\mathbf{z}_n^{(j)} \triangleq \big[z_{1,n}^{(j)}, \dots, z_{M_n^{(j)},n}^{(j)}\big]^{\mathrm{T}}$ at position $\mathbf{x}_n$ are connected to the features $k \in \mathcal{K}_n^{(j)}$ at positions $\mathbf{a}_{k,n}^{(j)}$. It is also possible that a measurement $z_{m,n}^{(j)}$ did not originate from any feature (false alarm, clutter) or that a feature did not give rise to any measurement (missed detection). The probability that a feature is detected is denoted by $s_{k,n}^{(j)}$. The distribution of false alarm measurements $f_{\mathrm{FA}}\big(z_{m,n}^{(j)}\big)$ is modeled as uniform on the region of interest,

i.e., the distance interval $[0, cT]$, where T is the measurement duration. The number of false alarms is modeled by a Poisson distribution with mean $\mu^{(j)}$. We assume that at any time n, each feature can generate at most one measurement, and each measurement can be generated by at most one feature [14], [23]. Possible associations between the agent and a feature at time n are described by the $K_n^{(j)}$-dimensional random vector $\mathbf{c}_n^{(j)} = \big[c_{1,n}^{(j)}, \ldots, c_{K_n^{(j)},n}^{(j)}\big]^{\mathrm{T}}$, whose k-th entry is defined as

$$c_{k,n}^{(j)} = \begin{cases} m \in \mathcal{M}_n^{(j)}, & \text{at time } n, \text{ feature } (j,k) \\ & \text{generates mesurement } z_{m,n}^{(j)} \\ 0, & \text{at time } n, \text{ feature } (j,k) \\ & \text{does not generate any} \\ & \text{measurement.} \end{cases} \tag{2}$$

We also define $\mathbf{c}_n \triangleq \big[\mathbf{c}_n^{(1)\mathrm{T}}, \ldots, \mathbf{c}_n^{(J)\mathrm{T}}\big]^{\mathrm{T}}$ and $\mathbf{c} \triangleq [\mathbf{c}_1^{\mathrm{T}}, \ldots, \mathbf{c}_n^{\mathrm{T}}]^{\mathrm{T}}$. As previously proposed in [16], [19], we can alternatively introduce a *measurement-oriented association vector* $\mathbf{b}_n^{(j)} = \big[b_{1,n}^{(j)}, \ldots, b_{M,n}^{(j)}\big]^{\mathrm{T}}$ with

$$b_{m,n}^{(j)} = \begin{cases} k \in \mathcal{K}_n^{(j)}, & \text{measurement } z_{m,n}^{(j)} \text{ is} \\ & \text{generated by feature } (j,k) \\ 0, & \text{measurement } z_{m,n}^{(j)} \text{ is not} \\ & \text{generated by any feature.} \end{cases} \tag{3}$$

We also define $\mathbf{b}_n \triangleq \big[\mathbf{b}_n^{(1)\mathrm{T}}, \ldots, \mathbf{b}_n^{(J)\mathrm{T}}\big]^{\mathrm{T}}$ and and $\mathbf{b} \triangleq [\mathbf{b}_1^{\mathrm{T}}, \ldots, \mathbf{b}_n^{\mathrm{T}}]^{\mathrm{T}}$. The redundant formulation of the data association is the key feature of the method that leads to excellent scalability [19], [20] (see for Section IV-B).

B. Agent and Feature Statistics

We define $\phi\big(\mathbf{x}_n, \mathbf{y}_{k,n}^{(j)}\big) = \phi\big(\mathbf{x}_n, \mathbf{a}_{k,n}^{(j)}, r_{k,n}^{(j)}\big)$ as a probability density function (pdf) or BP message defined jointly for the agent state $\mathbf{x}_n$ and the augmented feature state $\mathbf{y}_{k,n}^{(j)} = [\mathbf{a}_{k,n}^{(j)\mathrm{T}}, r_{k,n}^{(j)}]^{\mathrm{T}}$. As shown in [19], [20], if $\phi\big(\mathbf{x}_n, \mathbf{y}_{k,n}^{(j)}\big)$ is normalized to one, i.e.,

$$\sum_{r_{k,n}^{(j)} \in 0,1} \int\!\!\int \phi\big(\mathbf{x}_n, \mathbf{a}_{k,n}^{(j)}, r_{k,n}^{(j)}\big) \mathrm{d}\mathbf{x}_n \mathrm{d}\mathbf{a}_{k,n}^{(j)} = \phi(0) + \phi(1) = 1$$

then $\phi(0) = \phi_{k,n}^{(j)}$ can be interpreted as the probability that the (j,k)-th feature does not exist and $\phi(1)$ as the probability that it does. The paired joint agent and augmented feature states $\mathbf{x}_n, \mathbf{y}_{k,n}^{(j)}$ are assumed to evolve independently according to Markovian state dynamics, i.e.

$$f\big(\mathbf{x}_n, \mathbf{y}_n | \mathbf{x}_{n-1}, \mathbf{y}_{n-1}\big) = f(\mathbf{x}_0) \prod_{n'=1}^{n} f\big(\mathbf{x}_{n'} | \mathbf{x}_{n'-1}\big) \prod_{j=1}^{J} \prod_{k=1}^{K_{n'}^{(j)}} \times f\big(\mathbf{y}_{k,0}^{(j)}\big) f\big(\mathbf{y}_{k,n'}^{(j)} | \mathbf{y}_{k,n'-1}^{(j)}\big), \tag{4}$$

where $f(\mathbf{x}_0)$ and $f(\mathbf{y}_{k,0}^{(j)})$ are the prior pdfs at time $n = 0$ and $f(\mathbf{y}_{k,n}^{(j)} | \mathbf{y}_{k,n-1}^{(j)})$ is the state-transition pdf of the (j,k)-th feature. In the case a feature (j,k) does not exist at time $n-1$, i.e. $r_{k,n-1}^{(j)} = 0$, then the probability of birth (that it exists at time n) is given by p_{b}. The feature state is then distributed according to the birth pdf $f_{\mathrm{b}}(\mathbf{a}_{k,n}^{(j)})$, which will be described in Section IV-C. Thus, $f(\mathbf{y}_{k,n}^{(j)} | \mathbf{y}_{k,n-1}^{(j)})$ is given as [19]

$$f\big(\mathbf{a}_{k,n}^{(j)}, r_{k,n}^{(j)} | \mathbf{a}_{k,n-1}^{(j)}, 0\big) = \begin{cases} (1-p_{\mathrm{b}}) f_{\mathrm{D}}\big(\mathbf{a}_{k,n}^{(j)}\big), & r_{k,n}^{(j)} = 0 \\ p_{\mathrm{b}} f_{\mathrm{b}}\big(\mathbf{a}_{k,n}^{(j)}\big), & r_{k,n}^{(j)} = 1, \end{cases} \tag{5}$$

where $f_{\mathrm{D}}(\mathbf{a}_{k,n}^{(j)})$ represents a "dummy pdf" which has to integrate up to 1 at the support of the feature states [19]. If the (j,k)-th feature existed at time $n-1$, i.e. $r_{k,n-1}^{(j)} = 1$, then the probability of survival (that it still exists at time n) is given as p_{s}. If it still exists it is distributed according to the transition pdf $f(\mathbf{a}_{k,n}^{(j)} | \mathbf{a}_{k,n-1}^{(j)})$ and therefore we have [19]

$$f\big(\mathbf{a}_{k,n}^{(j)}, r_{k,n}^{(j)} | \mathbf{a}_{k,n-1}^{(j)}, 1\big) = \begin{cases} (1-p_{\mathrm{s}}) f_{\mathrm{D}}\big(\mathbf{a}_{k,n}^{(j)}\big), & r_{k,n}^{(j)} = 0 \\ p_{\mathrm{s}} f\big(\mathbf{a}_{k,n}^{(j)} | \mathbf{a}_{k,n-1}^{(j)}\big), & r_{k,n}^{(j)} = 1. \end{cases} \tag{6}$$

C. Likelihood Function

Let us stack the distance measurement vectors $\mathbf{z}_n^{(j)}$, $j \in \{1, \ldots, J\}$ obtained from all the signal transmissions and MPC estimation procedures into the vectors $\mathbf{z}_n \triangleq \big[\mathbf{z}_n^{(1)\mathrm{T}}, \ldots, \mathbf{z}_n^{(J)\mathrm{T}}\big]^{\mathrm{T}}$ and $\mathbf{z} \triangleq [\mathbf{z}_1^{\mathrm{T}}, \ldots, \mathbf{z}_n^{\mathrm{T}}]^{\mathrm{T}}$. Further, we stack the number of measurements into the vector $\mathbf{m} \triangleq [\mathbf{m}_1^{\mathrm{T}}, \ldots, \mathbf{m}_n^{\mathrm{T}}]^{\mathrm{T}}$ with $\mathbf{m}_n \triangleq \big[M_n^{(1)}, \ldots, M_n^{(J)}\big]^{\mathrm{T}}$. The statistical dependence of the distance measurement vector $\mathbf{z}_n$ on the agent state vector $\mathbf{x}_n$, augmented feature state $\mathbf{y}_n$, the association $\mathbf{c}_n$ and the number of measurements $\mathbf{m}_n$ is described by the likelihood function $f(\mathbf{z}_n | \mathbf{x}_n, \mathbf{y}_n, \mathbf{c}_n, \mathbf{m}_n)$. Under commonly used assumptions about the statistics of the measurements [14], [23], the *global likelihood function* can be factored as

$$f(\mathbf{z}|\mathbf{x}, \mathbf{y}, \mathbf{c}, \mathbf{m}) = C(\mathbf{z}) \prod_{n'=1}^{n} \prod_{j=1}^{J} \prod_{k=1}^{K_{n'}^{(j)}} \times g\big(\mathbf{x}_{n'}, \mathbf{a}_{k,n'}^{(j)}, r_{k,n'}^{(j)}, c_{k,n'}^{(j)}, \sigma_{k,n}^{(j,i)}; \mathbf{z}_{n'}^{(j)}\big), \tag{7}$$

where $C(\mathbf{z})$ is a normalization constant and the *local likelihood factor* $g\big(\mathbf{x}_n, \mathbf{a}_{k,n}^{(j)}, r_{k,n}^{(j)}, c_{k,n}^{(j)}, \sigma_{k,n}^{(j,i)}; \mathbf{z}_n^{(j)}\big)$ is given as

$$g\big(\bullet, \bullet, 1, \bullet, \bullet; \mathbf{z}_n^{(j)}\big) = \begin{cases} \dfrac{f\big(z_{m,n}^{(j)} | \mathbf{x}_n, \mathbf{a}_{k,n}^{(j)}, \sigma_{k,n}^{(j,i)}\big)}{f_{\mathrm{FA}}\big(z_{m,n}^{(j)}\big)}, & c_{k,n}^{(j)} = m \\ 1, & \text{else} \end{cases}$$

$$g\big(\bullet, \bullet, 0, \bullet, \bullet; \mathbf{z}_n^{(j)}\big) = 1,$$

where $m \in \mathcal{M}_n^{(j)}$. Here, the likelihood function $f\big(z_{m,n}^{(j)} | \mathbf{x}_n, \mathbf{a}_{k,n}^{(j)}, \sigma_{k,n}^{(j,i)}\big)$ is related to a noisy measurement of the distance between agent position $\mathbf{p}_n$ and feature position $\mathbf{a}_{k,n}^{(j)}$. This measurement is modeled as

$$z_{m,n}^{(j)} = \|\mathbf{p}_n - \mathbf{a}_{k,n}^{(j)}\| + v_{k,n}^{(j)}, \tag{8}$$

where feature k is connected with measurement m via $c_{k,n}^{(j)} = m$ and $v_{k,n}^{(j)}$ is zero-mean Gaussian noise with standard deviation $\sigma_{k,n}^{(j,i)}$, $i \in \{1, \ldots, S\}$. The range standard deviation

$\sigma_{k,n}^{(j,i)} = e_i \sigma_{k,n}^{(j)}$ is a scaled version of range standard deviation $\sigma_{k,n}^{(j)}$ provided by the higher-level non-Bayesian estimator. Its purpose will be explained in Section III-D.

D. Detection Probability and Discrete Variance Switching

The (j,k)-th feature is detected with a time-varying detection probability $s_{k,n}^{(j)}$ [17]. As proposed in [17], we also assume that $s_{k,n}^{(j)}$ is a discrete random variable with finite support $\mathcal{S} = \{d_1, \ldots, d_S\}$, where $d_i \in (0,1]$ and $i \in \{1, \ldots, S\}$. The temporal evolution is modeled by a discrete Markov chain with transition matrix $\mathbf{S}^{(j)} \in (0,1]^{S \times S}$ and the transition probability mass function (pmf) is given by $p\big(s_{k,n}^{(j)} = d_i | s_{k,n-1}^{(j)} = d_{i'}\big) = \big[\mathbf{S}^{(j)}\big]_{i',i}$, with the standard definition $\sum_{i=1}^{S} \big[\mathbf{S}^{(j)}\big]_{i',i} = 1$. The factorized prior pmf of joint state $\mathbf{s}$ is given as [17]

$$p(\mathbf{s}) = \prod_{n'=1}^{n} \prod_{j=1}^{J} \prod_{k=1}^{K_{n'}^{(j)}} p\big(s_{k,0}^{(j)}\big) p\big(s_{k,n'}^{(j)} | s_{k,n'-1}^{(j)}\big), \tag{9}$$

where $p\big(s_{k,0}^{(j)}\big)$ is the initial detection pmf at time 0. We also define $\mathbf{s}_n^{(j)} = \big[s_{1,n}^{(j)}, \ldots, s_{K_n^{(j)},n}^{(j)}\big]^{\mathrm{T}}$, $\mathbf{s}_n \triangleq \big[\mathbf{s}_n^{(1)\mathrm{T}}, \ldots, \mathbf{s}_n^{(J)\mathrm{T}}\big]^{\mathrm{T}}$ and $\mathbf{s} \triangleq [\mathbf{s}_1^{\mathrm{T}}, \ldots, \mathbf{s}_n^{\mathrm{T}}]^{\mathrm{T}}$. In addition to every discrete value d_i we define a finite set of standard-deviation levels for the range measurements. These levels are based on the standard-deviation estimates of the higher-level non-Bayesian estimator $\sigma_{k,n}^{(j)}$, written as $\sigma_{k,n}^{(j,i)}$, with $e_i \in [1, E]$ and $E \geq 1$. This rather heuristic choice can be argued as the following: For high detection probability values the measurements are expected to be more reliable, i.e. low standard deviation and vice versa for low detection probability. This means that for highest detection probability, the scaling factor $e_i = 1$, and for the lowest detection probability, $e_i = E$, leading to a higher measurement standard-deviation.

E. Distribution of Feature- and Measurement-oriented Association Variables

Under commonly used assumptions, the joint prior pmf of $\mathbf{c}$, $\mathbf{b}$ and $\mathbf{m}$ given the agent states $\mathbf{x}$, the augmented feature states $\mathbf{y}$ and the detection probabilities $\mathbf{s}$ can be expressed as [14], [19]

$$p(\mathbf{c}, \mathbf{b}, \mathbf{m} | \mathbf{x}, \mathbf{y}, \mathbf{s}) = C(\mathbf{m}) \prod_{n'=1}^{n} \prod_{j=1}^{J} \prod_{k=1}^{K_{n'}^{(j)}} \tag{10}$$

$$\times\, h\big(\mathbf{x}_{n'}, \mathbf{a}_{k,n'}^{(j)}, r_{k,n'}^{(j)}, c_{k,n'}^{(j)}, s_{k,n'}^{(j)}; M_{n'}^{(j)}\big) \prod_{m=1}^{M_{n'}^{(j)}} \Psi\big(c_{k,n'}^{(j)}, b_{m,n'}^{(j)}\big)$$

where $C(\mathbf{m})$ is a normalization factor and

$$h\big(\mathbf{x}_n, \mathbf{a}_{k,n}^{(j)}, 1, c_{k,n}^{(j)}, s_{k,n}^{(j)}; M_n^{(j)}\big) = \begin{cases} \dfrac{s_{k,n}^{(j)}}{\mu^{(j)}}, & c_{k,n}^{(j)} = m \\ (1 - s_{k,n}^{(j)}), & \text{else} \end{cases}$$

$$h\big(\mathbf{x}_n, \mathbf{a}_{k,n}^{(j)}, 0, c_{k,n}^{(j)}, s_{k,n}^{(j)}; M_n^{(j)}\big) = 1(c_{k,n}^{(j)}),$$

where $m \in \mathcal{M}_n^{(j)}$ and $1(c)$ equals 1 if $c = 0$ and 0 otherwise. $\Psi\big(c_{k,n}^{(j)}, b_{m,n}^{(j)}\big) \in \{0,1\}$ is the exclusion indicator function defined as

$$\Psi\big(c_{k,n}^{(j)}, b_{m,n}^{(j)}\big) = \begin{cases} 0, & c_{k,n}^{(j)} = m,\ b_{m,n}^{(j)} \neq k \\ & \text{or } b_{m,n}^{(j)} = k,\ c_{k,n}^{(j)} \neq m \\ 1, & \text{else.} \end{cases} \tag{11}$$

The indicator function enforces that the (j,k)-th feature can generate at most one measurement, and vice versa a measurement at physical anchor j originates from at most one feature.

F. Problem Statement

The problem addresses Bayesian detection and estimation of the feature states $\mathbf{a}_{k,n}^{(j)}$ and joint estimation of the agent state $\mathbf{x}_n$ from all the past and present measurements of all the features $j \in \{1, \ldots, J\}$, i.e., from the total measurement vector $\mathbf{z} \triangleq \big[\mathbf{z}_1^{\mathrm{T}}, \ldots, \mathbf{z}_n^{\mathrm{T}}\big]^{\mathrm{T}}$. In a Bayesian sense, the agent posterior pdf $f\big(\mathbf{x}_n | \mathbf{z}\big)$ is calculated and used to estimate the state $\mathbf{x}_n$. More specifically, we will develop an approximate calculation of the minimum mean-square error (MMSE) estimator [24]

$$\hat{\mathbf{x}}_n^{\mathrm{MMSE}} \triangleq \int \mathbf{x}_n f\big(\mathbf{x}_n | \mathbf{z}\big)\, \mathrm{d}\mathbf{x}_n\,. \tag{12}$$

Furthermore, in order to determine the existence of a specific features, we rely on the posterior existence probabilities $p\big(r_{k,n}^{(j)} = 1 | \mathbf{z}\big)$, which can be obtained from the posterior pdfs of the augmented feature states, $f\big(\mathbf{y}_{k,n}^{(j)} | \mathbf{z}\big) = f\big(\mathbf{a}_{k,n}^{(j)}, r_{k,n}^{(j)} | \mathbf{z}\big)$, i.e.

$$p\big(r_{k,n}^{(j)} = 1 | \mathbf{z}\big) = \int f\big(\mathbf{a}_{k,n}^{(j)}, r_{k,n}^{(j)} = 1 | \mathbf{z}\big) \mathrm{d}\mathbf{a}_{k,n}^{(j)}. \tag{13}$$

Finally, the higher-level algorithm that determines the standard deviation $\sigma_{k,n}^{(j)}$ corresponding to each feature, requires knowledge of the most probable MPC-to-feature association. This is obtained by means of an approximation of the maximum a posteriori (MAP) detector [25]

$$\hat{c}_{k,n}^{(j)\,\mathrm{MAP}} \triangleq \underset{c_{k,n}^{(j)} \in \{1, \ldots, M_n^{(j)}\}}{\arg\max}\ p\big(c_{k,n}^{(j)} | \mathbf{z}\big). \tag{14}$$

We consider only MAP estimates for $p\big(\hat{c}_{k,n}^{(j)\,\mathrm{MAP}} | \mathbf{z}\big) > P_{\mathrm{th}}^{\mathrm{assoc}}$, where $P_{\mathrm{th}}^{\mathrm{assoc}}$ represents a constant threshold. The calculations in (12), (13), and (14) will be based on approximate calculations of the joint posterior pdfs $f\big(\mathbf{x}_n | \mathbf{z}\big)$ and $f\big(\mathbf{a}_{k,n}^{(j)}, r_{k,n}^{(j)} | \mathbf{z}\big)$, and the marginal posterior pmfs $p\big(c_{k,n}^{(j)} | \mathbf{z}\big)$ by means of an efficient BP message passing algorithm.

IV. BP Method For Multipath-assisted SLAM

A. Factorization of the Joint Posterior PDF

Using Bayes' rule and common independence assumptions [14], [23], the joint posterior pdf $f(\mathbf{x}, \mathbf{y}, \mathbf{c}, \mathbf{b}, \mathbf{s} | \mathbf{z})$ can be expressed up to a constant factor as

$$\begin{aligned} f(\mathbf{x}, \mathbf{y}, \mathbf{c}, \mathbf{b}, \mathbf{s} | \mathbf{z}) &= f(\mathbf{x}, \mathbf{y}, \mathbf{c}, \mathbf{b}, \mathbf{s}, \mathbf{m} | \mathbf{z}) \\ &\propto f(\mathbf{z} | \mathbf{x}, \mathbf{y}, \mathbf{c}, \mathbf{b}, \mathbf{s}, \mathbf{m}) f(\mathbf{x}, \mathbf{y}, \mathbf{c}, \mathbf{b}, \mathbf{s}, \mathbf{m}) \end{aligned} \tag{15}$$

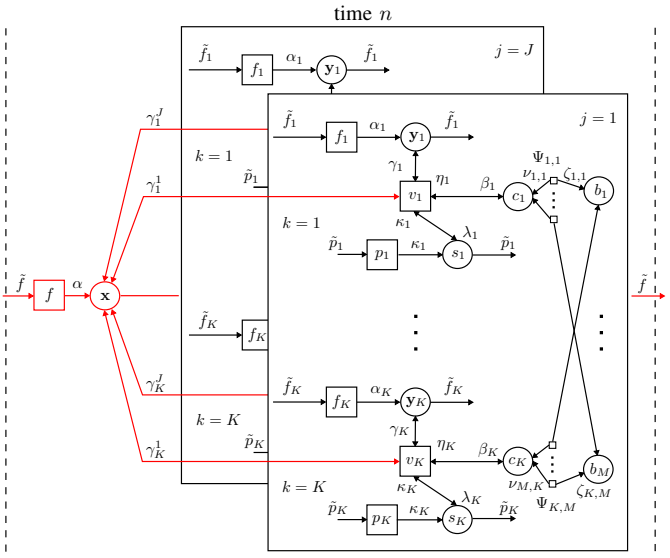

Fig. 2. Factor graph corresponding to the factorization in (16). The following short notations are used: $\mathbf{x} \triangleq \mathbf{x}_n$, $\mathbf{y}_k \triangleq \mathbf{y}_{k,n}^{(j)}$, $\alpha \triangleq \alpha(\mathbf{x}_n)$, $\alpha_k \triangleq \alpha(\mathbf{y}_{k,n}^{(j)})$, $\tilde{f} \triangleq \tilde{f}(\mathbf{x}_n)$, $\tilde{f}_k \triangleq \tilde{f}(\mathbf{y}_{k,n}^{(j)})$, $f \triangleq f(\mathbf{x}_n|\mathbf{x}_{n-1})$, $f_k \triangleq f(\mathbf{y}_{k,n}^{(j)}|\mathbf{y}_{k,n-1}^{(j)})$, $v_k \triangleq v(\mathbf{x}_n, \mathbf{a}_{k,n}^{(j)}, r_{k,n}^{(j)}, \sigma_{k,n}^{(j,i)}, c_{k,n}^{(j)}, s_{k,n}^{(j)}; \mathbf{z}_n^{(j)})$, $b_m \triangleq b_{m,n}^{(j)}$, $c_k \triangleq c_{k,n}^{(j)}$, $\Psi_{k,m} \triangleq \Psi(c_{k,n}^{(j)}, b_{m,n}^{(j)})$, $\beta_k \triangleq \beta(c_{k,n}^{(j)})$, $\eta_k \triangleq \eta(c_{k,n}^{(j)})$, $\nu_{m,k} \triangleq \nu_{m\to k}^{(p)}(c_{k,n}^{(j)})$, $\zeta_{k,m} \triangleq \zeta_{k\to m}^{(p)}(b_{m,n}^{(j)})$, $\gamma_k^j \triangleq \gamma_k^{(j)}(\mathbf{x}_n)$, $\gamma_k \triangleq \gamma(\mathbf{a}_{k,n}^{(j)}, r_{k,n}^{(j)})$, $p_k \triangleq p(s_{k,n}^{(j)}|s_{k,n-1}^{(j)})$, $s_k \triangleq s_{k,n}^{(j)}$, $\lambda_k \triangleq \lambda(s_{k,n}^{(j)})$, $\kappa_k \triangleq \kappa(s_{k,n}^{(j)})$, and $\tilde{p}_k \triangleq \tilde{p}(s_{k,n}^{(j)})$.

$$
\begin{aligned}
&= f(\mathbf{z}|\mathbf{x},\mathbf{y},\mathbf{c},\mathbf{m}) f(\mathbf{x},\mathbf{y},\mathbf{c},\mathbf{b},\mathbf{s},\mathbf{m}) \\
&= f(\mathbf{z}|\mathbf{x},\mathbf{y},\mathbf{c},\mathbf{m}) p(\mathbf{c},\mathbf{b}|\mathbf{z},\mathbf{s},\mathbf{m}) f(\mathbf{x},\mathbf{y}) p(\mathbf{s}),
\end{aligned}
$$

where the fact is used that $\mathbf{z}$ is conditionally independent of $\mathbf{s}$ given $\mathbf{c}$, that $\mathbf{c}$ and $\mathbf{b}$ are redundant and that $\mathbf{x}$ and $\mathbf{y}$ are independent of $\mathbf{s}$. By inserting (7) for $f(\mathbf{z}|\mathbf{x},\mathbf{y},\mathbf{c},\mathbf{m})$, (10) for $p(\mathbf{c},\mathbf{b},\mathbf{m}|\mathbf{x},\mathbf{y},\mathbf{s})$, (4) for $f(\mathbf{x},\mathbf{y})$ and (9) for $p(\mathbf{s})$, (15) is given as

$$
\begin{aligned}
f(\mathbf{x},\mathbf{y},\mathbf{c},\mathbf{b},\mathbf{s}|\mathbf{z}) \propto f(\mathbf{x}_0) \prod_{n'=1}^{n} \prod_{j=1}^{J} \prod_{k=1}^{K_{n'}^{(j)}} & p(s_{k,0}^{(j)}) f(\mathbf{y}_{k,0}^{(j)}) \\
&\times f(\mathbf{x}_{n'}|\mathbf{x}_{n'-1}) f(\mathbf{y}_{k,n'}^{(j)}|\mathbf{y}_{k,n'-1}^{(j)}) p(s_{k,n'}^{(j)}|s_{k,n'-1}^{(j)}) \\
&\times v(\mathbf{x}_{n'}, \mathbf{a}_{k,n'}^{(j)}, r_{k,n'}^{(j)}, \sigma_{k,n'}^{(j,i)}, c_{k,n'}^{(j)}, s_{k,n'}^{(j)}; \mathbf{z}_{n'}^{(j)}) \\
&\times \prod_{m=1}^{M_{n'}^{(j)}} \Psi(c_{k,n'}^{(j)}, b_{m,n'}^{(j)}),
\end{aligned} \tag{16}
$$

where $v(\bullet; \mathbf{z}_n^{(j)}) = g(\bullet; \mathbf{z}_n^{(j)}) h(\bullet; M_n^{(j)})$. This factorization of the joint posterior pdf is represented by the factor graph shown in Fig. 2. The red part represents all factors, variables, and messages concerning the agent state and the black part, factors, variables, and messages for all feature states.

B. BP Message Passing Algorithm

The proposed BP message passing scheme is an adaptation of the methods introduced in [15], [17], [19] to the factor graph in Fig. 2 based on the sum-product algorithm [26]. Since the factor graph contains loops, the presented method obtains only an approximation of the messages. The following scheduling is introduced for calculating the messages: (i) Message passing is only done forward in time, (ii) iterative message passing is executed for data association [16] and, (iii) iterative message passing is only executed once to consider the loops involving the agent state and the features. First, a prediction step is performed at time n. For the agent state, the prediction message is obtained as $\alpha(\mathbf{x}_n) = \int f(\mathbf{x}_n|\mathbf{x}_{n-1}) \tilde{f}(\mathbf{x}_{n-1}) \mathrm{d}\mathbf{x}_{n-1}$, where $\tilde{f}(\bullet)$ and $\tilde{p}(\bullet)$ defines messages calculated at the previous time $n-1$. The prediction message for the features reads

$$
\begin{aligned}
\alpha_k(\mathbf{a}_{k,n}^{(j)}, r_{k,n}^{(j)}) = & \sum_{r_{k,n-1}^{(j)} \in \{0,1\}} \int \tilde{f}(\mathbf{a}_{k,n-1}^{(j)}, r_{k,n-1}^{(j)}) \\
& \times f(\mathbf{a}_{k,n}^{(j)}, r_{k,n}^{(j)}|\mathbf{a}_{k,n-1}^{(j)}, r_{k,n-1}^{(j)}) \mathrm{d}\mathbf{a}_{k,n-1}^{(j)}.
\end{aligned}
$$

Finally, the prediction message for the detection probabilities is given as

$$
\kappa(s_{k,n}^{(j)}) = \sum_{i \in \mathcal{S}} p(s_{k,n}^{(j)}|s_{k,n-1}^{(j)} = d_i) \tilde{p}(s_{k,n-1}^{(j)} = d_i). \tag{17}
$$

Let us introduce the short notation $\int \alpha_k(\mathbf{a}_{k,n}^{(j)}, 0) \mathrm{d}\mathbf{a}_{k,n}^{(j)} \triangleq \alpha_{k,n}^{(j)}$. The following calculations are performed for all features $k \in \mathcal{K}_n^{(j)}$ of all physical anchors $j \in \mathcal{J}$ in parallel:

1) Measurement evaluation:

$$
\begin{aligned}
\beta(c_{k,n}^{(j)}) = & \sum_{i \in \mathcal{S}} \iint \kappa(s_{k,n}^{(j)} = d_i) \alpha_k(\mathbf{a}_{k,n}^{(j)}, 1) \alpha(\mathbf{x}_n) \\
& \times v(\mathbf{x}_n, \mathbf{a}_{k,n}^{(j)}, 1, \sigma_{k,n}^{(j,i)}, c_{k,n}^{(j)}, s_{k,n}^{(j)} = d_i; \mathbf{z}_n^{(j)}) \mathrm{d}\mathbf{x}_n \mathrm{d}\mathbf{a}_{k,n}^{(j)} \\
& + 1(c_{k,n}^{(j)}) \alpha_{k,n}^{(j)}.
\end{aligned}
$$

2) Iterative data association: Using $\beta(c_{k,n}^{(j)})$ the messages $\eta(c_{k,n}^{(j)})$ are computed by loopy BP. The messages $\nu_{m\to k}^{(p)}(c_{k,n}^{(j)})$ and $\zeta_{k\to m}^{(p)}(b_{m,n}^{(j)})$ are iterated for $p \in \{1, \ldots, P\}$, where P is the number of iterations [16], [17].

3) Agent measurement update:

$$
\begin{aligned}
\gamma_k^{(j)}(\mathbf{x}_n) = & \sum_{i \in \mathcal{S}} \sum_{c_{k,n}^{(j)}} \eta(c_{k,n}^{(j)}) \kappa(s_{k,n}^{(j)} = d_i) \int \alpha_k(\mathbf{a}_{k,n}^{(j)}, 1) \\
& \times v(\mathbf{x}_n, \mathbf{a}_{k,n}^{(j)}, 1, \sigma_{k,n}^{(j,i)}, c_{k,n}^{(j)}, s_{k,n}^{(j)} = d_i; \mathbf{z}_n^{(j)}) \mathrm{d}\mathbf{a}_{k,n}^{(j)} \\
& + \eta(c_{k,n}^{(j)} = 0) \alpha_{k,n}^{(j)}.
\end{aligned}
$$

4) Feature measurement update:

$$
\begin{aligned}
\gamma(\mathbf{a}_{k,n}^{(j)}, 1) = & \sum_{i \in \mathcal{S}} \sum_{c_{k,n}^{(j)}} \eta(c_{k,n}^{(j)}) \kappa(s_{k,n}^{(j)} = d_i) \\
& \times \int v(\mathbf{x}_n, \mathbf{a}_{k,n}^{(j)}, 1, \sigma_{k,n}^{(j,i)}, c_{k,n}^{(j)}, s_{k,n}^{(j)} = d_i; \mathbf{z}_n^{(j)}) \alpha(\mathbf{x}_n) \mathrm{d}\mathbf{x}_n,
\end{aligned}
$$

$$
\gamma(\mathbf{a}_{k,n}^{(j)}, 0) = \eta(c_{k,n}^{(j)} = 0) \triangleq \gamma_{k,n}^{(j)}.
$$

5) Detection probability update:

$$\lambda\big(s_{k,n}^{(j)}\big) = \sum_{c_{k,n}^{(j)}} \iint \kappa\big(s_{k,n}^{(j)}\big)\eta\big(c_{k,n}^{(j)}\big)\alpha_k\big(\mathbf{a}_{k,n}^{(j)},1\big)\alpha(\mathbf{x}_n) \times v\big(\mathbf{x}_n,\mathbf{a}_{k,n}^{(j)},1,\sigma_{k,n}^{(j,i)},c_{k,n}^{(j)},s_{k,n}^{(j)};\mathbf{z}_n^{(j)}\big)\mathrm{d}\mathbf{x}_n\mathrm{d}\mathbf{a}_{k,n}^{(j)} + \eta\big(c_{k,n}^{(j)}=0\big)\alpha_{k,n}^{(j)},$$

$$\tilde{p}\big(s_{k,n}^{(j)}\big) = \kappa\big(s_{k,n}^{(j)}\big)\lambda\big(s_{k,n}^{(j)}\big).$$

Now, we obtain the agent belief as $\tilde{f}\big(\mathbf{x}_n\big) = C_n\alpha(\mathbf{x}_n)\prod_{j\in\mathcal{J}}\prod_{k\in\mathcal{K}_n^{(j)}}\gamma_k^{(j)}\big(\mathbf{x}_n\big)$ and the beliefs for the augmented feature state as $\tilde{f}\big(\mathbf{a}_{k,n}^{(j)},1\big) = 1/C_{k,n}^{(j)}\alpha_k\big(\mathbf{a}_{k,n}^{(j)},1\big)\gamma\big(\mathbf{a}_{k,n}^{(j)},1\big)$ and $\tilde{f}_{k,n}^{(j)} = 1/C_{k,n}^{(j)}\gamma_{k,n}^{(j)}\alpha_{k,n}^{(j)}$ for $r_{k,n}^{(j)} = 0$. Note that C_n and $C_{k,n}^{(j)}$ are constant factors that are chosen such that the beliefs normalize to unity. Finally, beliefs for the association variables are obtained as $\tilde{p}\big(c_{k,n}^{(j)}\big) = \eta\big(c_{k,n}^{(j)}\big)\beta\big(c_{k,n}^{(j)}\big)$. These beliefs are used instead of $f\big(\mathbf{x}_n\big|\mathbf{z}\big)$ in (12), $f\big(\mathbf{a}_{k,n}^{(j)},r_{k,n}^{(j)}=1\big|\mathbf{z}\big)$ in (13), and $p\big(c_{k,n}^{(j)}\big|\mathbf{z}\big)$ in (14), respectively. Since a direct calculation of the beliefs is intractable, a particle-based approximation is used (see [20], [27] for details).

C. Birth of Features

The choice of the birth distribution introduced in the following is heuristic, but leads to good performance in multipath-assisted SLAM. The birth distributions consists of two parts: (i) It includes already existing features with low probability of existence and (ii) it considers entirely new features which have not been measured yet. The first part is given as

$$f_{\mathrm{b}}(\mathbf{y}_{k,n}^{(j)}) \triangleq \iint f\big(\mathbf{y}_{k,n}^{(j)}|\mathbf{y}_{k,n-1}^{(j)}\big)f(\mathbf{x}_n|\mathbf{x}_{n-1}) f_{\mathrm{b}}\big(\mathbf{y}_{k,n-1}^{(j)};\mathbf{z}_{n-1}^{(j)},\mathbf{x}_{n-1}\big)\mathrm{d}\mathbf{y}_{k,n-1}^{(j)}\mathrm{d}\mathbf{x}_{n-1},$$

where $f_{\mathrm{b}}\big(\mathbf{y}_{k,n-1}^{(j)};\mathbf{z}_{n-1}^{(j)},\mathbf{x}_{n-1}\big)$ is constructed from past measurements and the marginal association pmfs $p\big(c_{k,n-1}^{(j)} = m\big|\mathbf{z}_{n-1}\big)$ at agent state $\mathbf{x}_{n-1}$. The second part aims to introduce completely new features into the state space. This means that for every past measurement m at time $n-1$ that has a marginal association pmf $p\big(c_{k,n-1}^{(j)}=m\big|\mathbf{z}_{n-1}\big) < P_{\mathrm{th}}^{\mathrm{assoc}}$—the measurement could be clutter but more important also could originate from a potential new feature—a new state $\mathbf{y}_{K_n^{(j)}+1,n}^{(j)}$ is introduced.

V. Experimental Results

In this Section, the performance of the proposed method is analyzed based on simulations using real UWB measurement.

A. Measurement Setup

The measurements are taken from the seminar room scenario of the MeasureMINT database [28]. They correspond to two trajectories each consisting of 1000 agent positions with a 1 cm spacing as shown in Fig. 1 (gray lines). At each agent position, UWB radio channel measurements are available between the agent and two physical anchors at positions $\mathbf{a}_1^{(1)} = [0.5,7]^{\mathrm{T}}$ and $\mathbf{a}_1^{(2)} = [5.2,3.2]^{\mathrm{T}}$. The measurements were performed using an M-sequence correlative channel sounder with frequency range $3-10$ GHz. On the physical anchor and agent sides, dipole-like antennas (Euro-cent coins). These antennas have an approximately uniform radiation pattern in the azimuth plane and zeros in the directions of floor and ceiling. Within the total measured band, we selected the actual signal band using filtering with a root raised cosine pulse $s(t)$ with a roll-off-factor of 0.5 and two-sided 3 dB bandwidth of 2 GHz at a center frequency of $f_{\mathrm{c}} = 7$ GHz.

B. Experimental and Simulation Setup

The agent state transition pdf $f(\mathbf{x}_n|\mathbf{x}_{n-1})$, with $\mathbf{x}_n = [\mathbf{p}_n^{\mathrm{T}},\mathbf{v}_n^{\mathrm{T}}]^{\mathrm{T}}$, is defined by a 2-D linear constant-velocity motion model [29]. The driving noise $\mathbf{w}_n$ is independent across n, zero-mean, and Gaussian with covariance matrix $\mathbf{R}_w = \sigma_{\mathrm{w}}^2\mathbf{I}$. We chose $\sigma_{\mathrm{w}} = 0.02\,\mathrm{m/s}^2$. The features are assumed to be static and exposed to small state space noise, leading to $f\big(\mathbf{a}_{k,n}^{(j)}|\mathbf{a}_{k,n-1}^{(j)}\big) = \mathcal{N}\big(\mathbf{a}_{k,n-1}^{(j)},0.005^2\mathbf{I}\big)$.

We have estimated up to a maximum number of $M = 15$ MPCs per physical anchor. The range standard deviations $\sigma_{k,n}^{(j)}$ corresponding to the nonzero $\hat{c}_{k,n}^{(j)\mathrm{MAP}}$ were determined by a higher-level non-Bayesian algorithm that uses estimates of the complex MPC amplitudes of the last 30 time steps [22]. The false alarm PDF $f_{\mathrm{FA}}\big(z_{m,n}^{(j)}\big)$ is uniform on $[0\,\mathrm{m},40\,\mathrm{m}]$ and the mean number of false alarms ($c_{k,n}^{(j)}=0$) is $\mu^{(j)} = 5$. The set of detection probabilities $\mathcal{S} = \{0.1,0.2,\ldots,0.9\}$ with $|\mathcal{S}| = 9$ and the transition probabilities $\big[\mathbf{S}^{(j)}\big]_{i',i}$ are chosen according to [17], so that with probability 0.05, the detection probability is increased by 0.1, and with probability 0.1 it is decreased by 0.1. The standard deviation scaling is given by $|\mathcal{S}|$ uniformly spaced values on the interval $[1,E]$ with $E = 10$. The threshold probability for assuming measurements to be associated to features is $P_{\mathrm{th}}^{\mathrm{assoc}} = 0.01$ and the threshold for probability of existence of a feature is $P_{\mathrm{th}}^{\mathrm{e}} = 0.5$. For practicality, features below $P_{\mathrm{th}}^{\mathrm{e}}$ and with an SINR lower than 0 dB are deleted. The survival probability is $p_{\mathrm{s}} = 0.99$ and the birth probability is $p_{\mathrm{b}} = 0.3$. The reason why we choose a high birth probability is argued by the fact that for range-only measurements the estimator can converge to a wrong expected feature position. Therefore, the exploration of a new state region with the birth pdf is a remedy against this.

We use a sequential importance resampling particle filter implementation as presented in [20] with 8000 particles representing the survival pdf, 2000 representing the birth pdf of a feature, and 10000 for the agent state pdf. The number of loop iterations for data association is limited to $P = 1000$. *Prior knowledge*: The initial physical anchor states are drawn from 2-D Gaussian distributions $\mathbf{a}_{1,0}^{(1,2)} \sim \mathcal{N}\big(\mathbf{a}_1^{(1,2)},\mathrm{diag}\{0.1^2\}\big)$. The initial agent state $\mathbf{x}_0 \sim \mathcal{N}\big([\mathbf{p}_0,0,0]^{\mathrm{T}},\mathrm{diag}\{0.5^2,0.5^2,0.01^2,0.01^2\}\big)$, where $\mathbf{p}_0$ is the starting position of the trajectories.

C. Performance Results

Fig. 3 shows the empirical cumulative distribution function (CDF) of the agent position error $\Delta_n \triangleq \|\mathbf{p}_n - \hat{\mathbf{p}}_n\|$ along

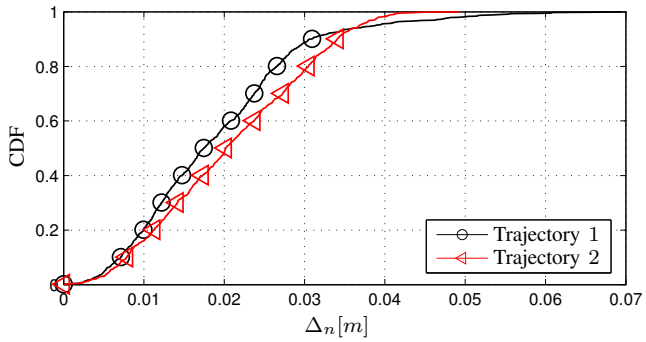

Fig. 3. CDF of the position error of the proposed method. Red lines indicate traj. 1 and black lines traj. 2 for two physical anchors at $\mathbf{a}_1^{(1)}$ and $\mathbf{a}_1^{(2)}$.

the two trajectories with 1000 agent positions. The red line illustrates the performance along traj. 1 and the black line along traj. 2. It can be seen that the proposed multipath-assisted SLAM algorithm is reaching a high level of accuracy very robustly. Since the CDFs all are converging to one at a reasonable error, none of the traj. runs can be seen as diverged, suggesting a high level of robustness of the proposed method. Further, the method reaches a reasonable VA-based feature representation of the environment. This was analyzed by comparing the VAs computed from the a-priori known floor plan with the estimated VAs.

VI. Conclusions and Future Perspective

In this paper we have proposed a new multipath-assisted feature-based SLAM algorithm based on probabilistic data association and BP message passing. The method is suited for highly cluttered measurements and with frequent birth and dead of tracked features. It shows high robustness in estimating the mobile agent state. Further, it provides a reasonable feature representation of an indoor environment using virtual anchors. Downsides of the method are (i) that the introduced birth mechanism is not Bayes optimal and (ii) that the estimation of the SINRs is non-Bayesian and decoupled from the SLAM filter, leaving space for future work. The next step we want to pursue is to adapt the marginal multi-Bernoulli/Possion filter [5] for deriving a closed-form description of unknown anchors and already known anchors, reaching Bayes optimality for our multipath-assisted SLAM method.

References

[1] H. Durrant-Whyte and T. Bailey, "Simultaneous localization and mapping: Part I," *IEEE Robot. Autom. Mag.*, vol. 13, no. 2, pp. 99–110, Jun. 2006.

[2] J. Mullane, B.-N. Vo, M. Adams, and B.-T. Vo, "A random-finite-set approach to Bayesian SLAM," *IEEE Trans. Robot.*, vol. 27, no. 2, pp. 268–282, Apr. 2011.

[3] ——, *Random Finite Sets for Robot Mapping & SLAM: New Concepts in Autonomous Robotic Map Representations*. Berlin, Germany: Springer, 2013.

[4] R. P. S. Mahler, *Statistical Multisource-Multitarget Information Fusion*. Norwood, MA, USA: Artech House, 2007.

[5] J. L. Williams, "Marginal multi-Bernoulli filters: RFS derivation of MHT, JIPDA, and association-based member," *IEEE Trans. Aerosp. Electron. Syst.*, vol. 51, no. 3, pp. 1664–1687, Jul. 2015.

[6] S. Reuter, B. T. Vo, B. N. Vo, and K. Dietmayer, "The labeled multi-Bernoulli filter," *IEEE Trans. Signal Process*, vol. 62, no. 12, pp. 3246–3260, Jun. 2014.

[7] T. Kropfreiter, F. Meyer, and F. Hlawatsch, "Sequential Monte Carlo implementation of the track-oriented marginal multi-Bernoulli/Poisson filter," in *Proc. FUSION-16*, Heidelberg, Germany, Jul. 2016, pp. 972–979.

[8] H. Deusch, S. Reuter, and K. Dietmayer, "The labeled multi-Bernoulli SLAM filter," *IEEE Signal Process. Lett.*, vol. 22, no. 10, pp. 1561–1565, Oct. 2015.

[9] E. Leitinger, P. Meissner, C. Rudisser, G. Dumphart, and K. Witrisal, "Evaluation of position-related information in multipath components for indoor positioning," *IEEE J. Sel. Areas Commun.*, vol. 33, no. 11, pp. 2313–2328, Nov. 2015.

[10] K. Witrisal, P. Meissner, E. Leitinger, Y. Shen, C. Gustafson, F. Tufvesson, K. Haneda, D. Dardari, A. F. Molisch, A. Conti, and M. Z. Win, "High-accuracy localization for assisted living: 5G systems will turn multipath channels from foe to friend," *IEEE Signal Process. Mag.*, vol. 33, no. 2, pp. 59–70, Mar. 2016.

[11] E. Leitinger, P. Meissner, M. Lafer, and K. Witrisal, "Simultaneous localization and mapping using multipath channel information," in *Proc. IEEE ICC-15*, London, UK, Jun. 2015, pp. 754–760.

[12] Y. Kuang, K. Astrom, and F. Tufvesson, "Single antenna anchor-free UWB positioning based on multipath propagation," in *Proc. IEEE ICC-13*, Budapest, Hungary, Jun. 2013, pp. 5814–5818.

[13] C. Gentner, T. Jost, W. Wang, S. Zhang, A. Dammann, and U. C. Fiebig, "Multipath assisted positioning with simultaneous localization and mapping," *IEEE Trans. Wireless Commun.*, vol. 15, no. 9, pp. 6104–6117, Sep. 2016.

[14] Y. Bar-Shalom and X.-R. Li, *Multitarget-Multisensor Tracking : Principles and Techniques*. Storrs, CT: Yaakov Bar-Shalom, 1995.

[15] E. Leitinger, F. Meyer, P. Meissner, K. Witrisal, and F. Hlawatsch, "Belief propagation based joint probabilistic data association for multipath-assisted indoor navigation and tracking," in *Proc. ICL-GNSS-16*, Barcelona, Spain, Jun. 2016.

[16] J. Williams and R. Lau, "Approximate evaluation of marginal association probabilities with belief propagation," *IEEE Trans. Aerosp. Electron. Syst.*, vol. 50, no. 4, pp. 2942–2959, Oct. 2014.

[17] F. Meyer, P. Braca, F. Hlawatsch, M. Micheli, and K. LePage, "Scalable adaptive multitarget tracking using multiple sensors," in *Proc. IEEE GLOBECOM-16*, Washington D.C., USA, Dec. 2016.

[18] E. Leitinger, "Cognitive Indoor Positioning and Tracking using Multipath Channel Information," Ph.D. dissertation, Graz University of Technology, 2016.

[19] F. Meyer, P. Braca, P. Willett, and F. Hlawatsch, "Tracking an unknown number of targets using multiple sensors: A belief propagation method," in *Proc. FUSION-16*, Heidelberg, Germany, Jul. 2016, pp. 719–726.

[20] ——, "A scalable algorithm for tracking an unknown number of targets using multiple sensors," *IEEE Trans. Signal Process.*, 2017, to appear.

[21] A. Molisch, "Ultra-wide-band propagation channels," *Proc. IEEE*, vol. 97, no. 2, pp. 353–371, Feb. 2009.

[22] P. Meissner, E. Leitinger, and K. Witrisal, "UWB for robust indoor tracking: Weighting of multipath components for efficient estimation," *IEEE Wireless Comm. Lett.*, vol. 3, no. 5, pp. 501–504, Oct. 2014.

[23] J. Vermaak, S. J. Godsill, and P. Perez, "Monte Carlo filtering for multi target tracking and data association," *IEEE Trans. Aerosp. Electron. Syst.*, vol. 41, no. 1, pp. 309–332, Jan. 2005.

[24] S. Kay, *Fundamentals of Statistical Signal Processing: Estimation Theory*. Upper Saddle River, NJ, USA: Prentice Hall, 1993.

[25] ——, *Fundamentals of Statistical Signal Processing: Detection Theory*. Upper Saddle River, NJ, USA: Prentice Hall, 1998.

[26] F. Kschischang, B. Frey, and H.-A. Loeliger, "Factor graphs and the sum-product algorithm," *IEEE Trans. Inf. Theory*, vol. 47, no. 2, pp. 498–519, Feb 2001.

[27] F. Meyer, O. Hlinka, H. Wymeersch, E. Riegler, and F. Hlawatsch, "Distributed localization and tracking of mobile networks including noncooperative objects," *IEEE Trans. Signal Inf. Process. Netw.*, vol. 2, no. 1, pp. 57–71, Mar. 2016.

[28] P. Meissner, E. Leitinger, M. Lafer, and K. Witrisal, "MeasureMINT UWB database," www.spsc.tugraz.at/tools/UWBmeasurements, 2013.

[29] X. R. Li and V. P. Jilkov, "Survey of maneuvering target tracking. Part I. Dynamic models," *IEEE Trans. Aerosp. Electron. Syst.*, vol. 39, no. 4, pp. 1333–1364, Oct. 2003.